NMR studies of 4-methylimidazole binding to cytochrome c: effects of methyl substituent on the binding affinity, the orientation of the ligand plane, and the electronic structure of the heme †

Yong Yao,[a] Yibing Wu,[a,b] Chengmin Qian[a] and Wenxia Tang *[a]

[a] Coordination Chemistry Institute, State Key Laboratory of Coordination Chemistry, Nanjing University, Nanjing 210093, P.R. China. E-mail: wxtang@netra.nju.edu.cn
[b] National Laboratory of Biomacromolecules, Institute of Biophysics, Academic Sinica, Beijing 100101, P. R. China

The binding of 4-methylimidazole (mim) to cytochrome c (cyt c) has been studied by ¹H NMR spectroscopy. The kinetic and thermodynamic parameters for the reaction were calculated. The assignment of a number of signals has led to the determination of the magnetic susceptibility tensor of mim–cyt c. It turned out that the orientation of the imidazole ring of mim was different from that of Him in Him–cyt c. This difference was due to the steric interaction between the 4-methyl and the surrounding peptides in the heme cavity. The pseudocontact and contact shifts of the four heme methyl groups in mim–cyt c were calculated. The hyperfine shift pattern and heme electron structure of mim–cyt c were compared with those of native cyt c and Him–cyt c.

Introduction

The magnetic properties of heme proteins have been studied extensively with the aim of obtaining insights into protein structure, the control of redox potential, and the mechanism of electron transfer. Horse cytochrome c (cyt c) has been one of the most extensively studied heme proteins using NMR methods. The magnetic susceptibility tensor of native cyt c has been well established and the dipole shifts have been calculated to separate the Fermi contact shifts of several groups bound to the heme.[1–3] This showed that the delocalization of the unpaired electron is essentially restricted to the heme, the sulfur of the axial Met ligand, and the ring of the other axial His ligand. Theoretical calculations concluded that both axial ligands (His/Met) were important, but that the Met chirality predominated in determining the electronic structure of the heme.[3]

cyt c can bind a wide range of ligands such as cyanide, azide, imidazole (Him) and pyridine (py) which displace Met-80 and ligate to the heme iron.[4–8] Studies of these ligand–cyt c complexes help to obtain insight into the structural aspects of the heme cavity and the asymmetric electron spin density distributions. The binding of imidazole to cyt c has been studied in detail[6,9–11] and recently the solution structure of Him–cyt c has been determined using the NMR method.[12] Those results showed that the two Him planes form an angle of 8° and the orientation of the co-ordinated Him relative to His-18 determined the in-plane orientation of the magnetic susceptibility tensor.[12] Considering that imidazole methyl derivatives will have more severe perturbation on the heme cavity than imidazole, in this paper, we used 4-methylimidazole (mim) as a probe to elucidate the effect of the methyl substituent on the binding affinity, imidazole plane orientation and electronic structure of the heme center.

Experimental

Sample preparation

Horse heart cyt c (type VI) was purchased from Sigma

Chemical Co. and purified as previously described.[13] 4-Methylimidazole was bought from ACROS ORGANICS and used without purification. The NMR samples consisted of 4 mM cyt c (for one-dimensional spectra), 6 mM cyt c and 100 mM mim (for one-dimensional and EXSY (exchange spectroscopy) experiments), or 4 mM cyt c containing 1 M mim (for one-dimensional, DQF (double quantum filtered) COSY and NOESY experiments) in D_2O. The pH of the samples was adjusted to 7.0 by addition of small volumes of DCl. The pH readings were not corrected for the isotope effect.

NMR spectroscopy

All the ¹H NMR experiments were performed on a Bruker AM 500 spectrometer equipped with an Aspect 3000 computer system. Typically, 16 K data points over a sweep width of 35.7 kHz were obtained for one-dimensional spectra. For two-dimensional spectra 512 × 2048 time domain data with a sweep width of 35.7 or 7.57 kHz in F_2 dimension were used, applying 128–160 scans for each t_1 increment. The carrier was centered on the residual water peak which was suppressed by presaturation during the relaxation delay. Chemical shift values are referenced to 1,4-dioxane at δ 3.74.

2-D NMR experiments including EXSY, DQF-COSY and TPPI (time proportional phase incrementation)-NOESY spectra were carried out using standard methods and phase cycling procedures. The detection of 2-D EXSY spectra was achieved using the standard NOESY pulse sequence with a mixing time of 25 or 50 ms. The NOESY spectra were recorded with a mixing time of 20 ms. Raw data were multiplied in both dimensions by shifted sine-squared window functions and Fourier transformed to obtain 1 K × 1 K real data points. A polynomial baseline correction was applied in both directions. Data processing was performed using the standard Bruker software package XWINNMR. The 2-D maps were analysed with the aid of the program XEASY.[14]

The integral values of the two-dimensional peaks were obtained by direct reading from the spectra using a square frame, and normalized according to $\Sigma I_{ij} = 1$. The same frame was used to estimate the average noise integral value in order to remove the noise effect from the quantitative two dimensional integration, and I_{ij} were corrected before normalization. The

DOI: 10.1039/b005577h

J. Chem. Soc., Dalton Trans., 2000, 4069–4074 **4069**

equilibrium magnetization values were obtained by integration of the one-dimensional spectra and also normalized.

Kinetics

For a system involving chemical exchange between two sites it has been shown that the peak amplitude in the EXSY spectrum is related to the exchange rate constant k', the relaxation rate and the mixing time τ_m by expression (1),[15] where A and R are

$$A = \exp(-R\tau_m) \qquad (1)$$

given by the matrices (2) and (3). In A the quantity I_{ij} is the two

$$A = \begin{bmatrix} I_{11}/M_1 & I_{12}/M_2 \\ I_{21}/M_1 & I_{22}/M_2 \end{bmatrix} \qquad (2)$$

$$R = \begin{bmatrix} \rho_1 & -k_{-1}' \\ -k_1' & \rho_2 \end{bmatrix} \qquad (3)$$

dimensional peak amplitude measured and normalized and M_i is the equilibrium magnetization obtained from integration of the one dimensional spectra and also normalized. R can be directly calculated in expression (4) where X is the eigenvector matrix and $XDX^{-1} = A$.

$$R = -\frac{\ln A}{\tau_m} = -\frac{X(\ln D)X^{-1}}{\tau_m} \qquad (4)$$

In this paper, the binding of mim to cyt c can be represented by reaction (5). The magnetization exchange between the

$$\text{cyt c} + \text{mim} \underset{k_{-1}}{\overset{k_1}{\rightleftharpoons}} \text{mim–cyt c} \qquad (5)$$
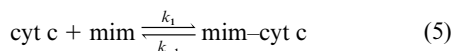
species is a first-order reaction (6). The relationships between

$$M_{\text{cyt c}} \underset{k_{-1}'}{\overset{k_1'}{\rightleftharpoons}} M_{\text{mim–cyt c}} \qquad (6)$$

the magnetization exchange rate constant k' and the exchange rate constant k can be found in eqns. (7a) and (7b), and the

$$k_1 = k_1'/[\text{mim}] \qquad (7a)$$

$$k_{-1} = k_{-1}' \qquad (7b)$$

apparent equilibrium constant K_{app} and the equilibrium constant K of the reaction can be calculated from eqns. (8a) and (8b) where k_a is the dissociation constant of mim. The

$$K_{\text{app}} = k_1/k_{-1} \qquad (8a)$$

$$K = K_{\text{app}} \{1 + ([\text{H}^+]/k_a)\} \qquad (8b)$$

thermodynamic values $\Delta H°$ and $\Delta S°$ of the reaction of cyt c with mim were obtained according to the Van't Hoff equation.

Magnetic susceptibility tensor

The hyperfine shift (δ_{hf}) includes contact (δ_{con}) and pseudocontact contributions (δ_{pc}).[3,16,17] The contact coupling is due to the presence of unpaired spin density on the resonating nucleus and vanishes a few chemical bonds away from the metal center. The pseudocontact contribution arises from the magnetic susceptibility anisotropy and depends on the nuclear position with respect to the principal axes of the magnetic susceptibility tensor. Based on the metal-centered point–dipole point–dipole approximation, eqn. (9) holds,[3] where $\Delta\chi_{\text{ax}}$ and $\Delta\chi_{\text{rh}}$ are the

$$\delta_{\text{pc}} = \frac{1}{12\pi r_i^3} [\Delta\chi_{\text{ax}}(3n_i^2 - 1) + \tfrac{3}{2}\Delta\chi_{\text{rh}}(l_i^2 - m_i^2)] \qquad (9)$$
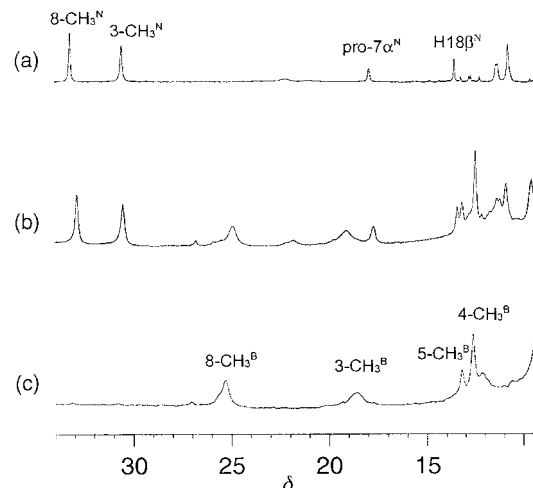
Fig. 1 Downfield hyperfine-shifted region of the ¹H NMR spectra in D₂O at 313 K, pH 7.0 of (a) native cyt c only, (b) cyt c with 100 mM mim and (c) cyt c with 1 M mim. Resonances due to cyt c and mim–cyt c are labelled with N and B respectively.

axial and rhombic anisotropies of the magnetic susceptibility, r_i is the distance of the nucleus i from the metal ion, and l_i, m_i, and n_i are the direction cosines of the position vector of atom i with respect to the principal axes of the magnetic susceptibility tensor.[17]

The pseudocontact shifts were calculated by subtracting the chemical shifts of reduced horse heart cyt c[12] from those of the mim-bound cyt c. The resonances of heme, of Cys-14 and -17, of His-18, of Met-80 and of bound mim would experience non-negligible contact shifts and therefore were not included in the calculations. The five independent parameters ($\Delta\chi_{\text{ax}}$, $\Delta\chi_{\text{rh}}$ and three direction cosines which define the principal directions of the tensor) were determined by fitting eqn. (9), using the solution structure of horse heart cyt c.[18]

Results and discussion

Binding of mim to cyt c

Fig. 1 presents the hyperfine-shifted region of ¹H NMR spectrum of cyt c at pH 7.0, 313 K in the presence of mim. It is obvious that the presence of mim significantly alters the hyperfine shifts which indicates the formation of a stable complex of cyt c with mim. For mim binding to cyt c at 315 K and pH 7.0 the chemical exchange is a two-site spin system. According to the theory of kinetics studied by means of exchange spectroscopy,[19,20] and as shown above, the reaction amplitude matrix A based on the integration of 8-CH₃ is obtained in eqn. (10). From matrix A the kinetic matrix R is calculated in

$$A = \begin{bmatrix} 0.758 & 0.195 \\ 0.366 & 0.740 \end{bmatrix} \qquad (10)$$

eqn. (11). Thus the magnetization exchange rate constants

$$R = \begin{bmatrix} 13.8 & -10.9 \\ -20.5 & 14.8 \end{bmatrix} \qquad (11)$$

$k_1' = 20.5$ s⁻¹ and $k_{-1}' = 10.9$ s⁻¹. According to eqns. (7a) and (7b) the reaction rate constants $k_1 = 204.5$ M⁻¹ s⁻¹ and $k_{-1} = 10.9$ s⁻¹. Then the equilibrium constants are calculated by eqns. (8a) and (8b): $K_{\text{app}} = 18.8$ M⁻¹ and $K = 38.4$ M⁻¹. Employing the same method, the kinetic and equilibrium data for binding of mim to cyt c at different temperatures were obtained and given in Table 1. The $\Delta H°$ and $\Delta S°$ for binding of mim to cyt c were obtained by least-squares fitting from Table 1 and listed in Table 2.

From Table 1 it follows that the rate constants for mim for the forward and reverse reactions increase with increasing temper-

Table 1 Rate and equilibrium constants for binding of mim to cyt c at different temperatures

T/K	$k_1/M^{-1} s^{-1}$	k_{-1}/s^{-1}	K_{app}/M^{-1}	K/M^{-1}
308	48.4	8.38	5.77	11.8
311	80.7	8.82	9.15	18.7
313	126	9.89	12.8	26.1
315	205	10.9	18.8	38.4

Table 2 Thermodynamic parameters of reactions of cyt c with Him and mim

Reaction	K/M^{-1}	$\Delta H^\circ/$ kJ mol^{-1}	$\Delta S^\circ/$ K^{-1} J mol^{-1}
Him and cyt c[9]	29.9 (311 K)	48.5	184
	37.2 (315 K)		
mim and cyt c	18.7 (311 K)	135	459
	38.4 (315 K)		

ature, and so does the equilibrium constant. This is similar to the case of imidazole binding to cyt c.[9] As to the equilibrium constant for this binding process (Table 2), we noticed that at relatively low temperature $K_{Him} > K_{mim}$, while at higher temperature $K_{mim} > K_{Him}$. The large temperature dependence of the equilibrium constant can be interpreted as follows. The pK_a of Him and mim are 6.95 and 7.37 respectively,[21] which means the binding ability of mim to cyt c should be stronger than that of Him. However, the methyl substituent weakens the binding by the steric hindering effect and overweighs the factor of pK_a. At relatively low temperature, the steric hindering effect dominates the binding process and results in a smaller equilibrium constant than that of Him binding to cyt c, while at higher temperature the much larger ΔS° (Table 2) resulting from the disorder nearby the heme, which is caused by the steric interaction between the 4-CH$_3$ and the surrounding residues, makes K_{mim} larger than K_{Him}.

As seen from Table 2, the ΔH° and ΔS° for binding of Him and mim to cyt c are both positive. Although $\Delta H^\circ > 0$ is unfavorable for the binding reactions, the positive ΔS° overweighs the negative effect of ΔH°. It can be calculated that when $T = 303$ K or above, both reactions have negative ΔG°. This suggests that the reaction is driven by a favorable entropy change and the affinity of Him and mim for cyt c arises from the positive ΔS°. However, the values of ΔH° and ΔS° for the binding of mim to cyt c are larger than those of Him.[9] Previous studies had shown that the binding of Him to cyt c not only induced the movements of some residues near the heme, but also caused disruption of some secondary structure elements of cyt c.[12] Since positive ΔH° arises from steric interactions of the bound ligand with the protein[22] and ΔS° represents the increased disorder after the binding reaction, the much larger ΔH° and ΔS° are ascribed to the more severe perturbation of the heme pocket with mim than Him. Moreover, the release of solvent molecules ordered around the more hydrophobic mim contributes to a larger entropy increase than with Him.

Assignments of some resonances of mim–cyt c

As most of the resonances of cyt c have been assigned,[18,23,24] the 2-D EXSY method can be used to determine the corresponding resonance assignments of mim–cyt c. In order to observe cross peaks due only to chemical exchange and to minimize the NOEs, short mixing times (25 and 50 ms) were used to record the EXSY spectra. The well resolved heme methyl groups of mim–cyt c can easily be assigned in the 2-D EXSY spectrum. However, for resonances of amino residues the results of a 2-D correlated experiment (DQF-COSY) were combined to delineate scalar connectivities and identify the assignments.
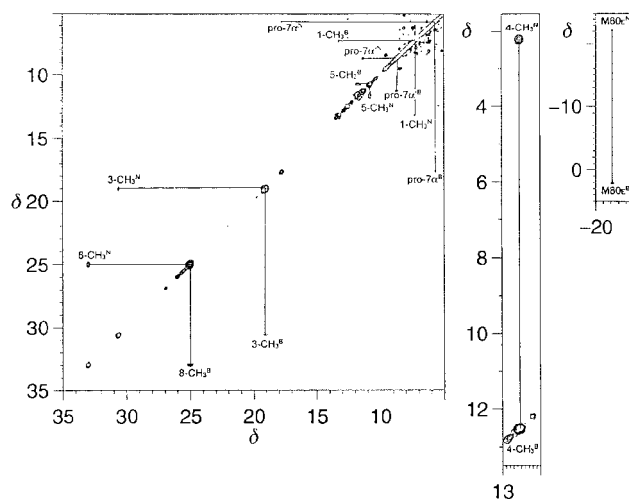
Fig. 2 Portions of the EXSY spectrum of cyt c with 100 mM mim at pH 7.0 and 313 K, mixing time 25 ms. Labelling as in Fig. 1.
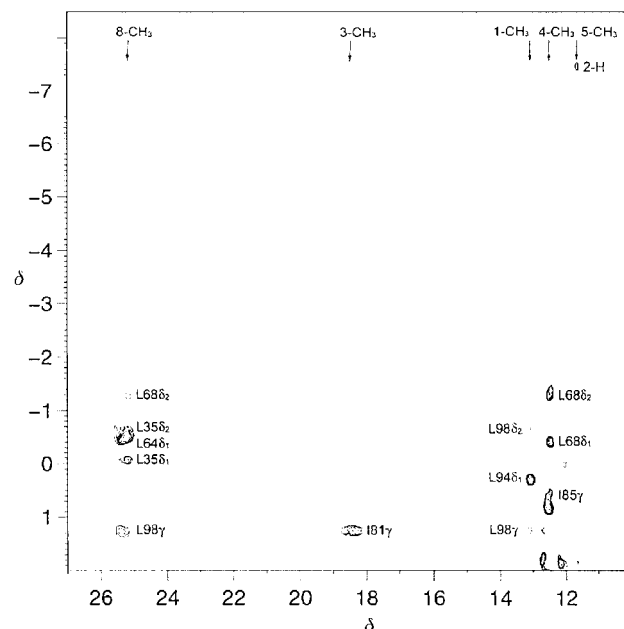
Fig. 3 Portions of the NOESY spectrum of cyt c with 1 M mim at pH 7.0 and 313 K, mixing time 20 ms.

An EXSY cross peak was clearly detected between 8-CH$_3$ of the native form and the resonance at δ 25.01 (Fig. 2). Other EXSY cross peaks have been observed at $\delta = 19.05$ for 3-CH$_3$, δ 13.24 for 1-CH$_3$, and δ 11.70 for 5-CH$_3$. The 7-Hα protons were assigned at δ 8.66 and δ 5.65. A well resolved signal (δ -1.23) was assigned to the thioether-2 methyl protons of mim–cyt c. The ϵ-CH$_3$ of Met-80 gives an EXSY cross peak with a signal at δ 2.04 which is the corresponding signal for the mim adduct. The αH of His-18 was identified at δ 9.50. An exchange cross peak was observed between one β-CH$_2$ signal at δ 7.92 in the native form[23] and that at δ 8.42 in mim–cyt c. The resonances of the other β-CH$_2$ proton in the mim-bound and unbound forms are too close to each other to resolve the EXSY connectivity. The resonance was identified at δ 13.22 in a NOESY experiment. A strong cross peak is observed at δ 12.53 and δ 2.28. As the signal at δ 2.28 is due to the resonance of the 4-CH$_3$ of the unbound mim, the signal at δ 12.53 then was assigned to the 4-CH$_3$ of the bound mim in the adduct. A peak at δ -7.43 is observed to have NOE with 5-CH$_3$ (Fig. 3). According to its large hyperfine shift and previous study of Him–cyt c,[9] it was assigned as 2-H of the bound mim. The assignments of the heme peripheral protons and some protons of His-18, Met-80, and bound mim are summarized in Table 3.

Table 3 Shift values of the hyperfine shifted signals of mim–cyt c (pH 7.0, T 313 K)

Assignment	δ
8-CH$_3$	25.01
3-CH$_3$	19.05
1-CH$_3$	13.24
5-CH$_3$	11.70
7-Hα	8.66
7-Hα'	5.65
Thioether-2	−1.23
His-18-α	9.50
His-18-β	13.22
His-18-β'	8.42
Met-80-ε	2.04
4-CH$_3$	12.53
2-H	−7.43

Table 4 Shift values for some residues in mim–cyt c (pH 7.0, T 313 K)

Assignment	δ		
	γH	δ_1H$_3$	δ_2H$_3$
Leu-35	0.40	−0.06	−0.45
Leu-64	0.87	−0.44	−0.56
Leu-68	1.18	−0.53	−1.31
Leu-94	0.75	0.24	−0.08
Leu-98	1.26	−0.12	−0.54
	γH	γH$'$	δH$_3$
Ile-9	1.20	0.61	0.39
Ile-57	0.86	0.74	0.15
Ile-75	1.99	0.79	−0.28
Ile-81	0.80	1.24	0.36
Ile-85	1.02	0.78	0.41
Ile-95	1.48	0.89	0.67
	βH	γ_1H$_3$	γ_2H$_3$
Val-3	2.00	0.91	0.88
Val-11	2.06	1.08	0.90
Val-20	1.97	0.78	0.62
	αH	α'H	
Gly-1	3.92	3.64	
Gly-6	3.93	3.08	
Gly-23	4.17	3.79	
Gly-24	4.32	3.78	
	αH	βH	β'H
Asn-2	4.83	2.78	2.45
Asn-70	5.47	3.30	3.04
	βH	γH$_3$	
Thr-19	5.37	2.17	
Thr-28	3.35	0.04	
Thr-78	6.20	2.82	
Thr-89	3.96	1.12	
	αH	βH$_3$	
Ala-15	5.32	1.82	
Ala-96	3.74	1.16	
Ala-101	3.90	0.56	
	C$_5$H	C$_6$H	C$_7$H
Trp-59	6.38	5.99	7.00
	(o)	(m)	(p)
Phe-10	6.93	7.13	
Phe-36	6.94	6.49	6.52
Phe-82	8.06	7.02	6.38
	(o)	(m)	
Tyr-74	7.42	6.92	

The method for assignments of the side-chain of some other residues first involved identification of the spin system belonging to a particular amino acid residue. This was done with the help of the DQF-COSY spectra which provided different fine-structure patterns for different spin systems. The second stage involved assignment of an amino acid spin system identified for a specific residue in the protein sequence with the aid of the 2-D EXSY spectra. The results are reported in Table 4.

NOE analysis and estimation of the mim plane orientation

NOE experiments can provide data on internuclear distances which are directly correlated with the molecular conformation. In paramagnetic systems, NOEs are relatively difficult to observe because of the intrinsic short T_1. However, the para-magnetism quenches spin diffusion allowing the selective detection of primary NOEs for large proteins.[25,26] The resulting NOEs reflect an internuclear distance approximately <5 Å for the protons on the pocket residues.[27] To elucidate the conformation changes occurring in the substitution of Met-80 by mim, it is necessary to examine the NOEs between the heme and certain residues, and between several residues and the bound mim.

Fig. 3 shows the NOESY spectrum of mim at pH 7.0 with a mixing time 20 ms. Some NOEs are observed between the four methyls and the surrounding amino residues: 8-CH$_3$ shows NOEs with Leu-98γH, Leu-68δ_2-CH$_3$, Leu-64δ_1-CH$_3$, Leu-35δ_1-CH$_3$ and Leu-35δ_2-CH$_3$; 3-CH$_3$ has NOEs with Ile-81γH; 1-CH$_3$ is observed to have NOEs with Leu-98δ_2-CH$_3$, Leu-94δ_1-CH$_3$ and Leu-98γH; and 5-CH$_3$ shows NOEs with 2-H of the bound mim. Inspection of the Him–cyt c solution structure reveals that the distances between heme methyls and most protons mentioned above are within NOE distance (<5 Å).[12] However, the mean distance between Leu-98γH and 8-CH$_3$ in Him–cyt c is 7.5 Å[12] and the two groups have strong NOE in mim–cyt c, which suggests that Leu-98γH becomes closer to 8-CH$_3$ in mim–cyt c compared to Him–cyt c.

The hyperfine shifts of the heme methyl resonances of several heme proteins have recently been analysed through a heuristic equation[28] that correlates the hyperfine shifts with the orientation of the iron axial ligands. This eqn. (12) is based on

$$\delta_i = \cos\beta[A\sin^2(\theta_i - \varphi) + B\cos^2(\theta_i + \varphi) + C] + D\sin\beta \quad (12)$$

pseudocontact shifts and contact shifts, where δ_i is the hyperfine shift of the ith methyl, θ_i the angle between the Fe–Me$_i$ direction and the iron–pyrrole II nitrogen (NB) axis, β the acute angle between the two histidine planes, φ the angle between the bisector of the angle β and the Fe–NB direction and A, B, C and D are constants, determined by fitting data on similar systems and with known structure. The experimental shifts of the present adduct would provide φ of 60° and β of 46°. Then the

two imidazole planes have angles of about 37 (for His-18) and 83° (for mim) counterclockwise to the Fe–NB direction respectively (Fig. 4).

The 4-CH$_3$ of the bound mim in mim–cyt c shows NOEs with δ-CH$_3$ of Leu-68 and Ile-85 (Fig. 3), and 2-H has NOEs with 5-CH$_3$. With the known structure of cyt c[18] and Him–cyt c,[12] the orientation of the mim plane was estimated to be along
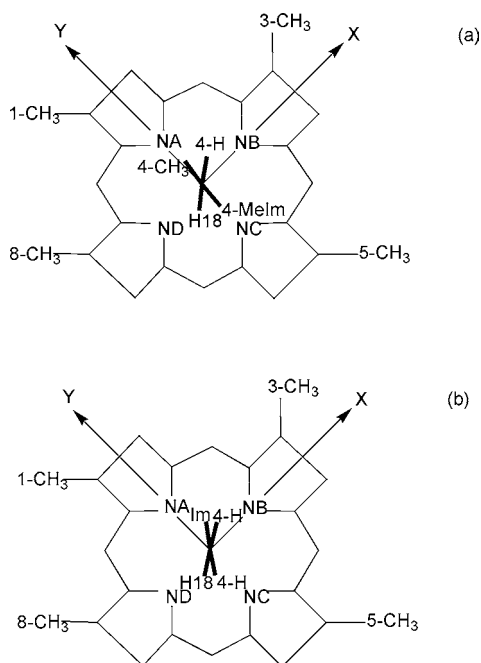
Fig. 4 Schematic representation of the orientations of the axial ligands relative to the heme moiety in (a) mim–cyt c and (b) Him–cyt c.

the Fe–NA direction, which fits well the values calculated by the heuristic equation.

It is interesting to compare the axial ligand orientation of this adduct with those of the imidazole–cyt c complex. In the latter the two imidazole planes have angles of about 41 and 49° counterclockwise to the Fe–NB direction respectively, and form an angle of about 8° (Fig. 4).[12] The His-18 seems to conserve its orientation after the binding of Him or mim (with an angle of 40° for cyt c,[18] 41° for Him–cyt c[12] and 37° for mim–cyt c counterclockwise to the Fe–NB direction), while the orientations of exogenous ligands Him and mim differ noticeably. In Him–cyt c the two rings have the 4-H in opposite directions[12] while in mim–cyt c, 4-CH₃ of mim and 4-H of His-18 are in the same direction (Fig. 4). Molecular mechanics calculations have shown that the parallel conformation is more stable than the perpendicular one in a bis-imidazole heme complex.[29] However, unlike Him–cyt c, the two imidazole rings in mim–cyt c form a much bigger angle of about 46°. This is probably owing to the space hindering effect between the 4-methyl group and the surrounding amino acid residues, which results in large $\Delta H°$ and $\Delta S°$ for the binding reaction.

Determination of the magnetic susceptibility tensor

The shift values of the assigned resonances reported in Table 4 allowed us to calculate the magnetic susceptibility tensor parameters for the mim–cyt c. The tensor has $\Delta\chi_{ax}$ and $\Delta\chi_{rh}$ values of 2.79×10^{-32} and -0.71×10^{-32} m³, respectively. The principle z axis of the magnetic anisotropy tensor forms an angle about 6° to the perpendicular to the heme plane whereas the x axis makes an angle of about 66° clockwise to the Fe–NB direction. The magnetic susceptibility tensor of the present system is similar to that of Him–cyt c.[12] The latter has values of $\Delta\chi_{ax}$ and $\Delta\chi_{rh}$ of 2.70×10^{-32} and -0.85×10^{-32} m³. The principal z axis of the magnetic anisotropy tensor in Him–cyt c forms an angle of 9° with respect to the perpendicular to the heme plane and the x axis forms an angle of 52° with the Fe–NB direction.

The orientation of the magnetic anisotropy tensor is directly linked to that of the two axial ligands. It is expected that the bisector between the projections of the two imidazole planes on the heme ring makes with the Fe-NB direction an angle of the same value but opposite sign with respect to that made by the x

Table 5 Pseudocontact (δ_{pc}) and contact shift values (δ_{con}) calculated for mim–cyt c and Him–cyt c at 313 K

Group	mim–cyt c		Him–cyt c[12]	
	δ_{pc}	δ_{con}	δ_{pc}	δ_{con}
8-CH₃	−2.89	25.76	−2.98	25.76
3-CH₃	−2.12	17.33	−2.11	15.68
1-CH₃	−4.30	14.05	−4.48	11.27
5-CH₃	−4.49	12.58	−4.60	14.63

direction of the χ tensor.[12,30] This fits well the calculation using the heuristic equation. In mim–cyt c the bisector of the two planes makes an angle of 60° with the Fe–NB direction as described above, while the x axis of the tensor forms an angle of 66° with the opposite direction.

Hyperfine shift pattern and temperature dependence of mim–cyt c

Native cyt c has a pairwise pattern for the heme methyl shifts.[3,31] The two most-shifted methyl resonances are 8-CH₃ and 3-CH₃, and the other two are 5-CH₃ and 1-CH₃ (8-CH₃ > 3-CH₃ ≫ 5-CH₃ > 1-CH₃). This hyperfine pattern is due to the contribution of Met-80 which imparts a pairwise pattern to the heme methyl groups on opposite pyrrole rings.[3] Upon binding of mim to cyt c, Met-80 is detached from the iron and the heme methyl shift pattern changes significantly. The heme methyl resonances of mim–cyt c have a much smaller spread of 13.29 ppm compared to 26.66 ppm for cyt c. The most shifted pair of heme methyls in cyt c shifts upfield while the other pair shifts downfield and their order changes to 8-CH₃ > 3-CH₃ > 1-CH₃ > 5-CH₃. This results in the disappearance of the pairwise pattern, which indicates that this complex has higher symmetry for the electron spin distribution relative to cyt c.

In comparison with Him–cyt c,[9–12] there is some difference between the chemical shift pattern of the heme methyls of mim–cyt c. The former complex shows a hyperfine-shifted pattern 8-CH₃ > 3-CH₃ > 5-CH₃ > 1-CH₃, while for the latter the pattern is 8-CH₃ > 3-CH₃ > 1-CH₃ > 5-CH₃. The pseudocontact and contact shifts of the four heme methyl groups in mim–cyt c and Him–cyt c are calculated and listed in Table 5. The four methyls of the two complexes seem to have similar pseudocontact shifts. However, the contact shifts of most methyl groups (except for 8-CH₃) of the two complexes are different, which primarily reflects a redistribution of the delocalized spin density among the four pyrroles. In cyt c the orientation of the axial Met is believed to determine the hyperfine shifts, while in the Him–cyt c and mim–cyt c complexes it is the orientation of the axial His and the corresponding bound exogenous ligand that determine the hyperfine shift. As the 4-methyl group has strong steric interaction with the surrounding polypeptide near the heme, mim adopts a different orientation from that of imidazole in mim–cyt c as discussed above and thus results in the different hyperfine shift pattern from Him–cyt c.

The temperature dependence of the heme methyl resonances for mim–cyt c is illustrated in Fig. 5, from which it can be concluded that all of the four heme methyls obey Curie's law. It has been reported that the shifts of 1-CH₃ and 5-CH₃ of native cyt c have an anti-Curie effect, which increases with increasing temperature, while 8-CH₃ and 3-CH₃ exhibit normal Curie behavior.[32,33] The temperature dependence of hyperfine shifts is related to the energy separation between the ground and excited levels, which, in turn, is modulated by interactions between the iron and the axial ligands.[3] In cyt c and mim–cyt c it is the axial perturbation that determines the heme electronic structure. The disparate temperature dependencies observed for heme methyls in native cyt c and mim–cyt c are therefore attributed to the change of the energy separation of the two electronic states upon complexation and the change in heme ligands. Previous
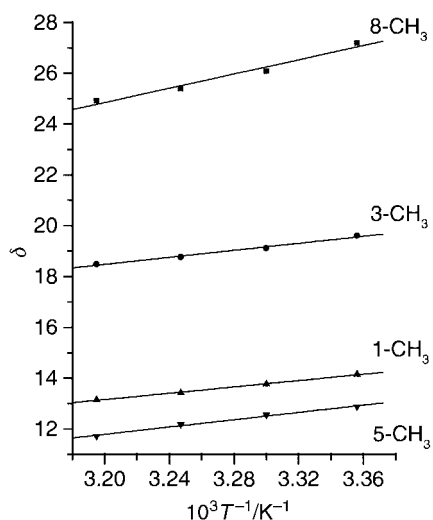
Fig. 5 Curie plots for mim–cyt c at pH 7.0.

research has found that the energy splitting in cyt b$_5$ can be estimated by $\Delta E \approx 5 \cos \beta$ kJ mol^{-1}, where β represents the angle between the two His ligands.[34] It can thus be concluded that the orientation of the mim ring is a crucial factor in the temperature dependence of the four heme methyl groups.

References

1 D. L. Turner, *Eur. J. Biochem.*, 1993, **211**, 563.
2 Y. Feng, H. Roder and S. W. Englander, *Biochemistry*, 1990, **29**, 3494.
3 G. N. La Mar, J. D. Satterlee and J. S. De Ropp, *NMR of Hemoproteins*, Academic Press, New York, 2000.
4 N. Sutin and J. K. Yandell, *J. Biol. Chem.*, 1972, **247**, 6932.
5 P. D. Baker and A. G. Mauk, *J. Am. Chem. Soc.*, 1992, **114**, 3619.
6 W. Shao, H. Sun, Y. Yao and W. Tang, *Inorg. Chem.*, 1995, **34**, 680.
7 D. Ma, J. Lu and W. Tang, *Biochim. Biophys. Acta*, 1998, **1384**, 32.
8 X. Hong and D. W. Dixson, *FEBS Lett.*, 1989, **246**,106.
9 W. Shao, J. Wei and W. Tang, *Acta Chim. Sin.*, 1992, **50**, 1129.
10 G. Liu, W. Shao, X. Huang, H. Wu and W. Tang, *Biochim. Biophys. Acta*, 1996, **1127**, 61.
11 W. Shao, G. Liu, X. Huang, H. Wu and W. Tang, *Biochim. Biophys. Acta*, 1996, **1295**, 44.
12 L. Banci, I. Bertini, G. Liu, J. Lu, T. Reddig, W. Tang, Y. Wu and D. Zhu, unpublished work.
13 D. L. Bautigan, S. Ferguson-miller and E. Margolish, *Methods Enzymol.*, 1978, **53D**, 128.
14 C. Eccles, P. Güntert, M. Billeter and K. Wüthrich, *J. Biomol. NMR*, 1991, **1**, 111.
15 R. R. Ernst, G. Bodenhausen and A. Wokaun, *Principles of Nuclear Magnetic Resonances in One and Two Dimensions*, Oxford University Press, 1987.
16 I. Bertini, P. Turano and A. J. Vila, *Chem. Rev.*, 1993, **93**, 2833.
17 L. Banci, I. Bertini, K. L. Bren, M. A. Cremonini, H. B. Gray, C. Luchinat and P. Turano, *J. Biol. Inorg. Chem.*, 1996, **1**, 117.
18 L. Banci, I. Bertini, H. B. Gray, C. Luchinat, T. Reddig, A. Rosato and P. Turano, *Biochemistry*, 1997, **36**, 9867.
19 E. R. Johnston, M. J. Dellwo and J. Hendrix, *J. Magn. Reson.*, 1986, **66**, 399.
20 E. W. Abel, T. P. J. Coston, K. G. Orrell, V. Sik and D. Stephenson, *J. Magn. Reson.*, 1986, **70**, 34.
21 D. D. Perrin, *Dissociation Constants of Organic Bases in Aqueous Solution*, IUPAC, London, 1965.
22 M. M. M. Saleem and M. T. Wilson, *Inorg. Chim. Acta*, 1988, **153**, 105.
23 G. Williams, G. R. Moore, R. Porteous, M. N. Robinson, N. Soffe and R. J. P. Williams, *J. Mol. Biol.*, 1985, **183**, 763.
24 Y. Feng, H. Roder, S. W. Englander, A. J. Wang and D. L. Di Stefano, *Biochemistry*, 1989, **28**, 195.
25 V. Thanabal, J. S. De Ropp and G. N. La Mar, *J. Am. Chem. Soc.*, 1987, **109**, 265.
26 L. B. Dugad, G. N. La Mar and S. W. Unger, *J. Am. Chem. Soc.*, 1990, **112**, 1386.
27 S. J. McLachlan, G. N. La Mar and E. Sletten, *J. Am. Chem. Soc.*, 1986, **108**, 1285.
28 I. Bertini, C. Luchinat, G. Parigi and F. A. Walker, *J. Biol. Inorg. Chem.*, 1999, **4**, 515.
29 L. A. Herbert, F. George, P. A. James, J. C. Arthur, W. D. Michael, T. H. Barbara and C. R. Douglas, *Acta Crystallogr.*, *Sect. D*, 1994, **50**, 596.
30 N. V. Shokhirev and F. A. Walker, *J. Am. Chem. Soc.*, 1998, **120**, 981.
31 K. L. Bren, H. B. Gray, L. Banci, I. Bertini and P. Turano, *J. Am. Chem. Soc.*, 1995, **117**, 8067.
32 H. Senn and K. Wüthrich, *Biochim. Biophys. Acta*, 1983, **743**, 69.
33 L. Banci, I. Bertini, C. Luchinat, R. Pierattelli, N. V. Shokhirev and A. A. Walker, *J. Am. Chem. Soc.*, 1998, **120**, 8472.
34 D. L. Turner, *Eur. J. Biochem.*, 1995, **227**, 829.